JOURNAL OF SOLID STATE CHEMISTRY 78, 108–116 (1989)

The Crystal and Magnetic Structures of Sr_2LuRuO_6, Ba_2YRuO_6, and Ba_2LuRuO_6

P. D. BATTLE* AND C. W. JONES

Department of Inorganic and Structural Chemistry, Leeds University, Leeds LS2 9JT, United Kingdom

Received June 3, 1988; in revised form August 22, 1988

Powder neutron diffraction data have been used to refine the crystal and magnetic structures of the ordered perovskites Sr_2LuRuO_6, Ba_2YRuO_6, and Ba_2LuRuO_6. Sr_2LuRuO_6 is monoclinic, with space group $P2_1/n$: $a = 5.7400(1)$, $b = 5.7375(1)$, $c = 8.1118(2)$ Å, $\beta = 90.16(1)°$. Ba_2YRuO_6 and Ba_2LuRuO_6 are cubic, with space group $Fm3m$: $a = 8.3390(5)$ and $8.2720(4)$ Å, respectively. All three compounds are Type I antiferromagnets at 4.2 K with an ordered magnetic moment of $\sim 2\ \mu_B$ per Ru^{5+}. High-temperature magnetic susceptibility data suggest that the Ru^{5+} d-electrons in all three compounds should be regarded as itinerant rather than localized. © 1989 Academic Press, Inc.

Introduction

The mixed metal oxides Ba_2LaRuO_6, Ca_2LaRuO_6, Ca_2YRuO_6, and Sr_2YRuO_6 all adopt perovskite-like structures with an ordered, alternate arrangement of cations on the octahedral (B) sites (*1–3*). In the case of Ba_2LaRuO_6 and Sr_2YRuO_6, the cations taking part in the ordering are Ru^{5+} and La^{3+} or Y^{3+}, respectively, whereas the ordering in Ca_2LaRuO_6 is between Ca^{2+} and Ru^{5+} and the formula can be more informatively written as $CaLa[CaRu]O_6$; the Ca^{2+} and La^{3+} ions on the 12-coordinate A site are disordered. The ordering in Ca_2YRuO_6 is best approximated by the representation $Ca_{1.5}Y_{0.5}[(Ca_{0.5}Y_{0.5})Ru]O_6$ and in this case there is no ordering between the Ca^{2+} and Y^{3+} ions on either the A or B sites. The crystal structures of all four compounds take a unit cell of dimension $\sim 5.5 \times \sim 5.5 \times \sim 8$ Å, that is $\sqrt{2}a_p \times \sqrt{2}a_p \times 2a_p$ where a_p is the size of the simple cubic perovskite unit cell. A fragment of a representative unit cell is shown in Fig. 1 to illustrate the way in which large octahedra containing an alkaline earth or lanthanide cation alternate with smaller octahedra containing Ru^{5+}. The space group symmetry of these oxides is monoclinic or lower and the octahedra are therefore rotated away from their ideal cubic orientation. The magnetic properties of these compounds are interesting for a number of reasons, but principally because the existing data suggest that the outer d-electrons on the transition metal ions are neither truly localized nor truly itinerant, but that their behavior is intermediate between these two extremes (*1, 4*). However, our present study was motivated by another aspect of the magnetic properties, that is the spin arrangement adopted in the low-temperature antiferromagnetic phase. Although the crystal structure is properly

* To whom correspondence should be addressed.

0022-4596/89 $3.00

Copyright © 1989 by Academic Press, Inc.
All rights of reproduction in any form reserved.

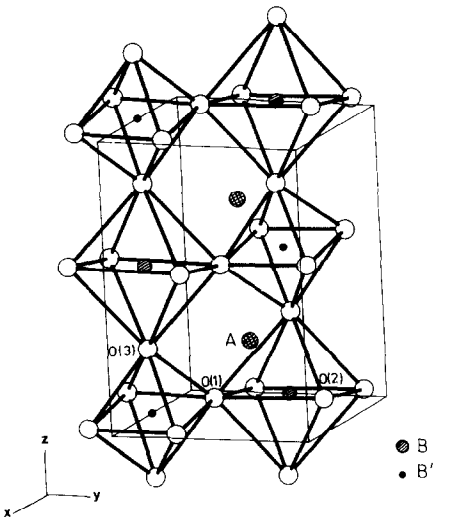

FIG. 1. The crystal structure of the ordered perovskites A_2BRuO_6.

described by the $(\sqrt{2} \times \sqrt{2} \times 2)a_p$ cell, it is convenient to discuss the magnetic structure in terms of a pseudocubic unit cell of size $2a_p \times 2a_p \times 2a_p$. In this setting (Fig. 2) the magnetic Ru^{5+} ions form a face centered array. There are two principal magnetic superexchange interactions in such a structure: that between nearest-neighbor (nn) Ru^{5+} ions, separated by a distance of $\sqrt{2}a_p$, and that between next-nearest-neighbor (nnn) Ru^{5+} ions separated by a distance of $2a_p$ along a pathway of the form Ru–O–*M*–O–Ru where *M* is a diamagnetic alkaline earth or lanthanide cation. If the strength of this latter interaction is negligible, then the array of Ru^{5+} ions is expected to show Type I spin ordering, as illustrated in Fig. 2a. However, if the strength of the nnn antiferromagnetic superexchange interaction is significant, but still less than the nn coupling, then a Type III (Fig. 2b) structure is predicted (*5*), and if the nnn interaction dominates that between nearest neighbors, then Type II ordering should occur (Fig. 2c). Of the systems studied to date, Sr_2YRuO_6, Ca_2YRuO_6, and Ca_2LaRuO_6 adopt the Type I structure, whereas Ba_2LaRuO_6 shows Type III ordering. It is thus clear that the superexchange interaction between nn is greater than that between nnn in all of these compounds, and that the strength of the latter interaction is insignificant in all except Ba_2LaRuO_6. Although the existence of a strong superexchange along the face diagonal of the $\sim 2a_p$ cube is consistent with the $t_{2g}^3 e_g^0$ electron configuration of the octahedrally coordinated Ru^{5+} ions, it is not clear why the strength of the nnn interaction should be greatest in Ba_2LaRuO_6. We originally suggested (*1*), in comparing this compound with CaLa[CaRu]O_6, that the vacant *5d* orbitals of La^{3+} are low enough in energy to take part in the superexchange process, whereas the *4p* orbitals on Ca^{2+} have too high an energy to do so. In order to test this hypothesis we have now prepared and characterized Ba_2YRuO_6 and Ba_2LuRuO_6. The introduction of Y and Lu is a means of increasing the electronegativity of the diamagnetic 6-coordinate cation and hence of decreasing the energy of the vacant outer orbitals at that site. If our original proposal was correct we would expect that the nnn superexchange in Ba_2YRuO_6 and Ba_2LuRuO_6 would be sufficiently strong to give rise to Type III, or possibly even Type II, ordering. We have also prepared and characterized Sr_2LuRuO_6 in order to provide a comparison with Sr_2YRuO_6.

Experimental

Polycrystalline samples of Ba_2YRuO_6, Ba_2LuRuO_6, and Sr_2LuRuO_6 were prepared by firing appropriate amounts of $BaCO_3$, $SrCO_3$, Y_2O_3, Lu_2O_3, and RuO_2 (all Johnson Matthey Chemicals) in a platinum crucible. The oxides were dried before use. The reaction mixtures were heated in pellet form at the following temperatures for several days, with frequent regrinding: Ba_2YRuO_6 and $SrLuRuO_6$ at 1350°C; Ba_2LuRuO_6 at

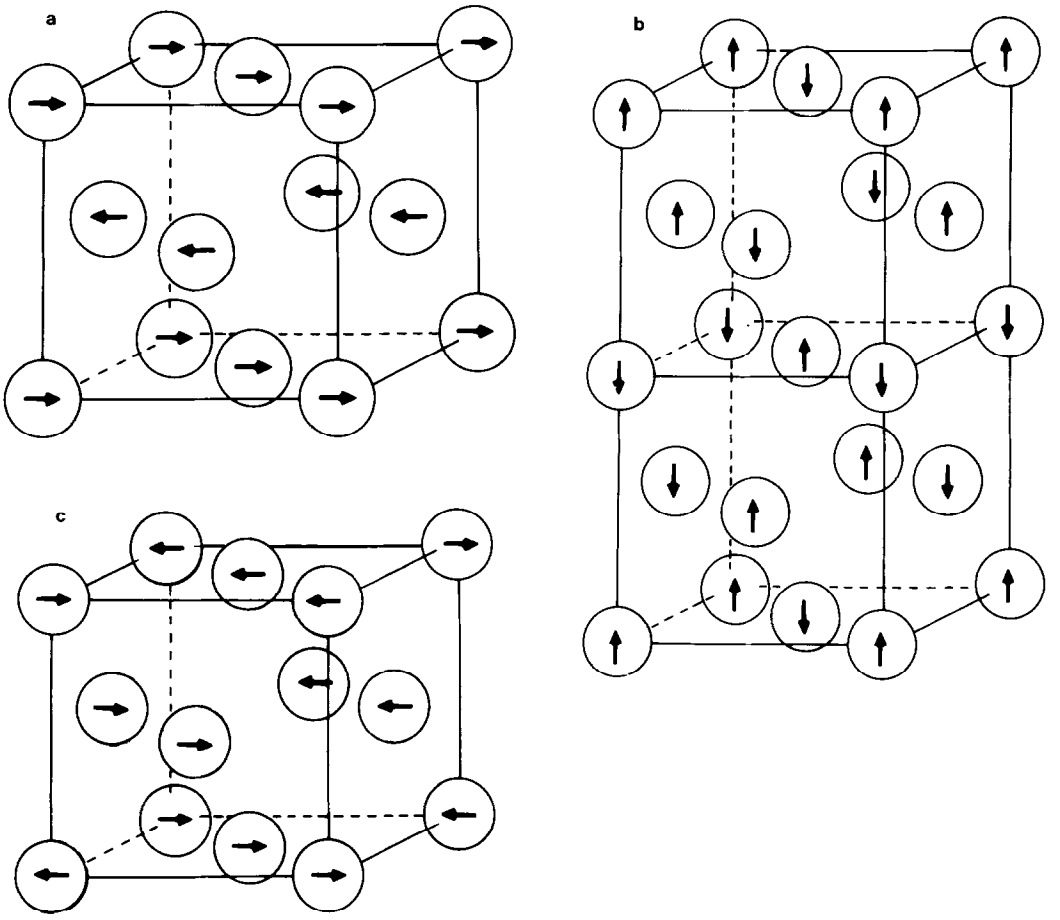

FIG. 2. The antiferromagnetic structures available to a face centered array of cations by (a) Type I, (b) Type III, and (c) Type II (only one octant of the unit cell is drawn).

1300°C. The products were shown to be perovskite-like single phase materials by the use of X-ray powder diffraction. Neutron diffraction data were collected on each sample at room temperature and 4.2 K using the diffractometer Dla at ILL Grenoble. A wavelength of 1.909 Å was used in all experiments, with the exception of those carried out at room temperature on Ba_2YRuO_6 and Sr_2LuRuO_6, for which a wavelength of 1.956 Å was used. Any error in these values was neglected in the calculation of unit cell parameters. The samples were contained in vanadium cans. Data were collected at 2θ intervals of 0.05° over the angular range $0 < 2\theta < 160°$, each experiment lasting approximately 9 hr. Magnetic susceptibility data were collected in the temperature range $80 < T < 300$ K using a Newport Instruments Gouy balance. The approximate Néel temperatures of Sr_2LuRuO_6 and Ba_2LuRuO_6 were measured by recording the neutron diffraction pattern as a function of temperature on the diffractometer D20 at ILL.

Results

(i) Room-temperature crystal structures. Our X-ray and neutron diffraction data both indicate that Ba_2YRuO_6 and Ba_2LuRuO_6

TABLE I

OBSERVED AND CALCULATED INTENSITY DATA FOR Ba_2YRuO_6 AND Ba_2LuRuO_6 AT ROOM TEMPERATURE

	Ba_2YRuO_6			Ba_2LuRuO_6		
{hkl}	I_{obs}	$\sigma(I_{obs})$	I_{calc}	I_{obs}	$\sigma(I_{obs})$	I_{calc}
111	496	44	396	352	36	248
200	7380	98	7660	3990	73	4320
220	5550	85	5950	3010	63	3250
311	149	27	112			
222	11300	126	11000	7130	94	7010
400	26200	174	26100	15400	132	15500
331	875	47	943	335	32	320
420	6170	91	5980	3690	71	3380
422	4000	76	3920	2180	55	2140
511/333	1790	56	1700	837	41	747
440	29000	181	28600	17200	140	16600
531	250	31	249	119	30	154
600/442	4800	85	4670	2510	60	2570
620	3690	78	3950	1710	53	1900
533	39	23	38			
622	10300	118	10400	6450	92	6510
444	15500	147	15200	8560	102	8510
711/551	2270	73	2250	958	46	940
640	3670	79	4120	1880	55	2040
642	7110	100	6890	3330	70	3190
731/553	3770	82	3550	1220	52	1280
800	13000	136	13500	6520	97	6860
733	3860	93	3950	1280	58	1230
820/644	9620	127	9430	4260	87	4180

have cubic symmetry at room temperature and the neutron data have been analyzed quantitatively in order to refine the crystal structures of the two materials. Refinements based on the integrated intensities of Bragg reflections were carried out in space group $Fm3m$ with a unit cell of approximate size $(2a_p)^3$, thus allowing for an ordered arrangement of cations over the B sites. A scale factor, four isotropic temperature factors, and the coordinates of the oxygen atom on the 24(e) site were refined using the intensities of 29 reflections spread over 24 diffraction maxima in the case of Ba_2YRuO_6 and the intensities of 27 reflections (22 maxima) in the case of Ba_2LuRuO_6. The refinements resulted in intensity-based R-factors at 2.65 and 3.42%, respectively. The

TABLE II

STRUCTURAL PARAMETERS FOR Ba_2MRuO_6 (M = Y OR Lu) AT ROOM TEMPERATURE (SPACE GROUP $Fm3m$)

M	Atom	Site	x	y	z	B (Å^2)
Y	Ba	8c	$\frac{1}{4}$	$\frac{1}{4}$	$\frac{1}{4}$	0.32(9)
	Y	4a	0	0	0	0.4(1)
	Ru	4b	$\frac{1}{2}$	0	0	0.2(1)
	O	24e	0.2657(3)	0	0	0.44(7)
Lu	Ba	8c	$\frac{1}{4}$	$\frac{1}{4}$	$\frac{1}{4}$	0.5(1)
	Lu	4a	0	0	0	0.6(2)
	Ru	4b	$\frac{1}{2}$	0	0	0.5(2)
	O	24e	0.2631(4)	0	0	0.61(9)

Note. Unit cell parameters: M = Y, a_0 = 8.3390(5) Å; M = Lu, a_0 = 8.2720(4) Å.

observed and calculated intensities are listed in Table I, the refined structural parameters are given in Table II, and bond lengths are presented in Table III. The diffraction pattern of Sr_2LuRuO_6 was more complex than those of Ba_2YRuO_6 and Ba_2LuRuO_6 and it was consequently necessary to use profile analysis (*6*) in order to refine the structure. A weighted profile R-factor of 7.27% resulted from the refinement of 257 Bragg reflections distributed over 2320 profile points, the corresponding intensity-based R-factor being 2.8%. In addition to the usual profile parameters, 18 atomic parameters were refined in space group $P2_1/n$ which also permits an ordered arrangement

TABLE III

BOND LENGTHS (IN Å) FOR Ba_2YRuO_6 AND Ba_2LuRuO_6 AT ROOM TEMPERATURE

Ba_2YRuO_6		Ba_2LuRuO_6	
Ru–O	1.954(3)	Ru–O	1.960(3)
Y–O	2.216(3)	Lu–O	2.176(3)
Ba–O	2.951(3)	Ba–O	2.927(3)

TABLE IV

STRUCTURAL PARAMETERS FOR Sr_2LuRuO_6 AT ROOM TEMPERATURE (SPACE GROUP $P2_1/n$)

Atom	Site	x	y	z	B (Å^2)
Sr	4*e*	0.0028(9)	0.0201(4)	0.2469(8)	0.36(3)
Lu	2*d*	½	0	0	0.21(8)
Ru	2*c*	½	0	½	0.27(8)
O1	4*e*	0.2635(7)	0.2914(9)	0.0326(6)	0.93(9)
O2	4*e*	0.2034(7)	−0.2285(8)	0.0339(5)	0.25(8)
O3	4*e*	−0.0574(8)	0.4901(6)	0.2388(5)	0.29(8)

Note. Cell parameters: $a = 5.7400(1)$, $b = 5.7375(1)$, $c = 8.1118(2)$ Å, $\beta = 90.16(1)°$.

TABLE V

BOND LENGTHS (IN Å) AND BOND ANGLES (IN DEGREES) FOR Sr_2LuRuO_6 AT ROOM TEMPERATURE

Lu–O1	2.170(8)		Ru–O1	1.946(8)	
Lu–O2	2.167(8)		Ru–O2	1.965(8)	
Lu–O3	2.144(8)		Ru–O3	1.967(8)	
Sr–O1		Sr–O2		Sr–O3	
2.78(1)		2.83(1)		2.72(1)	
2.91(1)		2.52(1)		2.57(1)	
2.59(1)		2.84(1)			
O3–Lu–O1	90.3		O3–Ru–O1	91.1	
O3–Lu–O2	91.3		O3–Ru–O2	90.8	
O1–Lu–O2	92.4		O1–Ru–O2	90.4	

of *B*-site cations but in a unit cell of size $\sqrt{2}a_p \times \sqrt{2}a_p \times 2a_p$. The background level was estimated by interpolation between regions of the profile where there were no Bragg peaks, and statistical variations in the background level were taken into account in assigning a weight to each profile point. The refined structural parameters are listed in Table IV and bond lengths and bond angles are given in Table V. The final observed, calculated, and difference diffraction profiles are plotted in Fig. 3. The following scattering lengths were used in all calculations: $b_{Ba} = 0.52$, $b_{Lu} = 0.73$, $b_O = 0.58$, $b_{Ru} = 0.73$, $b_{Sr} = 0.69$, $b_Y = 0.79 \times 10^{-12}$ cm. A full listing of the observed and calculated diffraction profiles of Sr_2LuRuO_6 is available from the authors.

(*ii*) *4.2 K crystal structures.* The neutron diffraction data sets collected at 4.2 K all contain low-angle Bragg peaks (exemplified

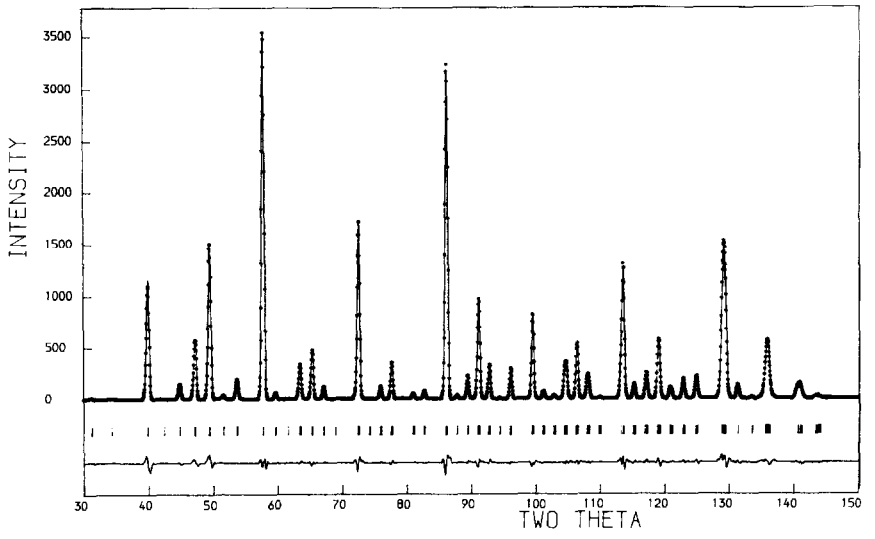

FIG. 3. The observed (. . .), calculated (—), and difference neutron diffraction profiles of Sr_2LuRuO_6 at room temperature. Reflection positions are marked.

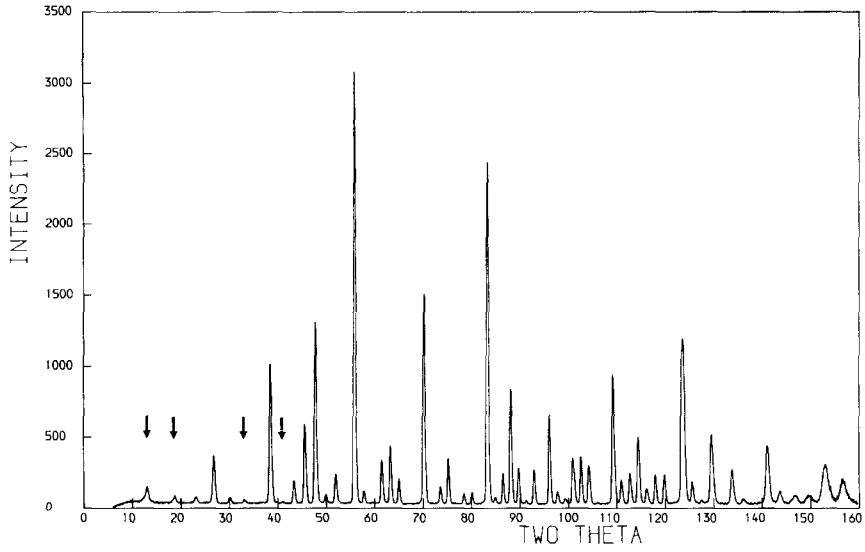

FIG. 4. The observed neutron diffraction profile for Sr_2LuRuO_6 at 4.2 K. Magnetic peaks indicative of Type I ordering are arrowed.

in Fig. 4 for Sr_2LuRuO_6) which are consistent with the presence of Type I antiferromagnetic ordering (Fig. 2a). The data were otherwise very similar to those collected at room temperature and the crystal structures were therefore refined in space groups $Fm3m$ (Ba_2YRuO_6 and Ba_2LuRuO_6) and $P2_1/n$ (Sr_2LuRuO_6) as described above. The resulting structural parameters are listed in Tables VI and VII. In order to estimate the magnitude of the ordered component of the magnetic moment we compared the intensity of the relatively strong, low-angle (001) magnetic peak to the intensities of several nuclear peaks, assuming a value of unity for the Ru^{5+} form factor at this low-Q value (sin $\theta/\lambda \sim 0.06$). The Ru^{5+} form factor is not sufficiently well known to warrant the inclusion in the analysis of the weaker magnetic peaks at higher Q values. The values derived for the ordered magnetic moment per Ru^{5+} ion, assuming a collinear magnetic structure, are given in Table VIII.

(iii) Magnetic susceptibilities 80 < T < 300 K. The inverse molar magnetic susceptibilities of Ba_2LuRuO_6, Ba_2YRuO_6, and Sr_2LuRuO_6 are plotted in Fig. 5. The values

TABLE VI

STRUCTURAL PARAMETERS FOR Ba_2MRuO_6 (M = Y OR Lu) AT 4.2 K (SPACE GROUP $Fm3m$)

M	a_0 (Å)	x_{24e}	R (%)
Y	8.3198(4)	0.2652(3)	2.6
Lu	8.2619(5)	0.2631(3)	2.3

TABLE VII

STRUCTURAL PARAMETERS FOR Sr_2LuRuO_6 AT 4.2 K (SPACE GROUP $P2_1/n$)

Atom	Site	x	y	z	B (Å^2)
Sr	4*e*	0.0056(8)	0.0254(4)	0.2472(6)	0.38(3)
Lu	2*d*	½	0	0	0.43(8)
Ru	2*c*	½	0	½	0.68(9)
O1	4*e*	0.2660(6)	0.2945(8)	0.0342(6)	1.00(10)
O2	4*e*	0.2017(7)	−0.2283(8)	0.0358(4)	0.28(7)
O3	4*e*	−0.0606(7)	0.4885(6)	0.2371(5)	0.64(8)

Note. a = 5.7130(1), b = 5.7180(1), c = 8.0762(2) Å, β = 90.19(1)° ($R_{(wpr)}$ = 8.5%, R_I = 3.9%).

TABLE VIII

MAGNETIC PARAMETERS OF Ba_2LuRuO_6, Ba_2YRuO_6, AND Sr_2LuRuO_6

Compound	θ (K)	T_N (K)	μ_{eff} (μ_B)	$\mu_{4.2\,K}$ (μ_B)
Ba_2LuRuO_6	−630(9)	35(1)	4.4(1)	2.06(6)
Ba_2YRuO_6	−630(9)	—	4.5(2)	2.11(6)
Sr_2LuRuO_6	−353(7)	30(1)	3.9(1)	2.10(8)

of the effective magnetic moment (μ_{eff}) and the Weiss constant (θ) derived from the graph are listed in Table VIII, as are the Neel temperatures determined in neutron diffraction experiments.

Discussion

The observation of cubic symmetry in Ba_2YRuO_6, the only one of the title compounds to have been reported previously, contradicts the work of Donohue and McCann (*7*), who prepared a phase of apparently hexagonal symmetry using a similar preparative method. X-ray powder diffraction patterns taken from our product before reaction was complete resembled those expected from a hexagonal material, and we therefore suggest that Donohue and McCann were working with an incompletely reacted mixture. The crystal chemistry of Ba_2LuRuO_6 is clearly similar to that of Ba_2YRuO_6, in the same way that Sr_2LuRuO_6 resembles Sr_2YRuO_6 (*2*). The Ru–O bond distances are very similar in all three of the materials described in this paper, and they are also similar to those reported previously for Ru^V oxides (*1–3*). The cubic phases contain perfectly regular RuO_6 octahedra of course, and even in monoclinic Sr_2LuRuO_6 the degree of distortion is small, as can be seen from the bond angles in Table V. This is to be expected for an ion with a $4d^3$ electron configuration on a 6-coordinate site. The Y–O bond length in Ba_2YRuO_6 is slightly longer than the average value (2.202 Å) found in Sr_2YRuO_6 but it is nevertheless a relatively short Y–O dis-

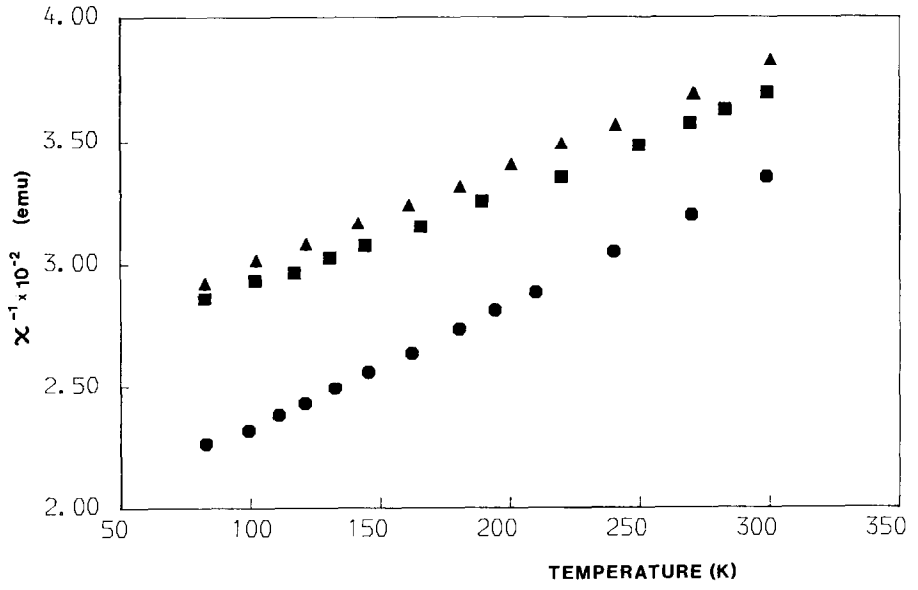

FIG. 5. The inverse molar magnetic susceptibilities of Ba_2LuRuO_6 (▲), Ba_2YRuO_6 (■), and Sr_2LuRuO_6 (●) as a function of temperature.

tance. The Lu–O bond lengths in Ba_2LuRuO_6 and Sr_2LuRuO_6 are similar and again they are short compared to the mean distances reported for other compounds containing LuO_6 octahedra, for example, $Ba_3Lu_4O_9$ (average = 2.22 Å) and $CaLu_2O_4$ (average = 2.24 Å), although the distorted octahedra in the latter two compounds do contain distances as short as 2.09 Å (*8, 9*). The absence of any departure from cubic symmetry in Ba_2YRuO_6 and Ba_2LuRuO_6 stems from the fact that the octahedral holes between the BaO_3 layers in the structure are large enough to accommodate an ordered arrangement of Ru and Lu/Y atoms without the layers being distorted. This is not the case when the layers have the composition SrO_3, nor when the ions to be accommodated between BaO_3 layers are Ru^{5+} and the larger La^{3+}, as in Ba_2LaRuO_6.

We have previously (*2*) concluded that the $4d^3$ electrons in Sr_2YRuO_6 are localized rather than itinerant, and that the degree of delocalization increases with decreasing unit-cell volume, and hence with decreasing Ru–Ru distance, along the series Sr_2YRuO_6, Ca_2LaRuO_6, and Ca_2YRuO_6 (*3*). These monoclinic materials all show Type I antiferromagnetic behavior at low temperatures. The results described above indicate that Sr_2LuRuO_6 fits this series well; the unit cell volume (267 Å^3) is intermediate between those of Sr_2YRuO_6 and Ca_2LaRuO_6 and the effective magnetic moment in the paramagnetic phase (3.9 μ_B) is also intermediate in magnitude, indicative of a degree of electron delocalization which is greater than that found in the Y-containing compound. A value of 3.9 μ_B is greater than the magnetic moment expected for a 6-coordinate d^3 ion from the second transition series, where spin–orbit coupling would normally reduce the observed moment below that predicted by the spin-only formula. The enhanced magnetic moment and also the high θ/T_N ratio, lead us to place Sr_2LuRuO_6 in the itinerant electron regime of the conceptual phase diagram proposed by Goodenough (*4*) for *d*-electron systems. However, it appears that this compound may lie closer to the localized/delocalized electron boundary than any of the Ru^{5+} oxides studied previously, those compounds, with the exception of Sr_2YRuO_6, having $\mu_{eff} > 4\ \mu_B$, consistent with extensive electron delocalization.

Unfortunately, the data relating to Ba_2YRuO_6 and Ba_2LuRuO_6 do not fit the simple model wherein the Ru–Ru distance is the single factor which determines the extent of delocalization. The unit cell volumes to be compared with the value of 267 Å^3 quoted above for Sr_2LuRuO_6 are 290 and 283 Å^3, respectively, and yet the magnetic data listed in Table VIII show convincingly that the outer *d*-electrons in these two compounds are not truly localized. We therefore suggest that the cubic symmetry, and the corresponding absence of any tilting of the RuO_6 octahedra, leads to an improved overlap of the Ru t_{2g} orbitals in neighboring RuO_6 polyhedra, and that this improved overlap compensates for the increase in the Ru–Ru distance. It has been argued (*10*) that the strength of the intercation interactions responsible for electron delocalization will increase with decreasing acidity of the *A*-site cation, that is on going from Sr-containing compounds to their Ba analogues. However, we have previously shown (*3*) that this is inconsistent with the observed properties of these Ru^V oxides. We now believe that delocalization is likely to be found in those compounds which have either a short Ru–Ru distance or a highly symmetrical crystal structure.

The observation of Type I magnetic ordering in all three of the title compounds at low temperatures disproves our hypothesis that the strength of the nnn superexchange will increase as the energy of the outer *d*-orbitals decreases. Thus Ba_2LaRuO_6 remains the only member of this family of compounds to show a significant nnn anti-

ferromagnetic superexchange interaction, and hence Type III ordering, in addition to the apparently dominant nn interaction which, when acting alone, leads to Type I ordering. We conclude that unit-cell volume is again the dominant parameter, and that as the unit cell expands, the strength of the nn interaction decreases more rapidly than that between nnn until the latter becomes a significant effect in Ba_2LaRuO_6 (volume = 312 Å^3). Divalent and trivalent ions larger than Ba^{2+} and La^{3+} would be needed to further increase the relative strength of the nnn interaction and produce Type II ordering. The ordered component of the magnetic moment is $\sim 2\ \mu_B$ for all materials studied, and is consistent with the presence of $Ru^{5+}: 4d^3$ ions, but with a substantial degree of covalency in the Ru–O bonds. This high level of covalency is consistent with the suggestion of a *d*-electron system which has moved out of the localized electron regime and yet is not completely delocalized, in which case we would not expect to observe long-range magnetic ordering (*4*). Finally, we should point out that it is somewhat unusual for a material to retain cubic symmetry while displaying Type I antiferromagnetism; we would have expected exchangestriction to produce a contraction along the axis perpendicular to the ferromagnetic sheets. It is possible that such a contraction does occur, but that the effect is too small to be detected in a neutron powder diffraction experiment.

Acknowledgments

We thank SERC for financial support and Dr. J. K. Cockcroft for experimental assistance at ILL Grenoble.

References

1. P. D. Battle, J. B. Goodenough, and R. Price, *J. Solid State Chem.* **46,** 234 (1983).
2. P. D. Battle and W. J. Macklin, *J. Solid State Chem.* **52,** 138 (1984).
3. P. D. Battle and W. J. Macklin, *J. Solid State Chem.* **54,** 245 (1984).
4. J. B. Goodenough, "Proceedings of the Robert A. Welch Foundation Conferences on Chemical Research XIV," Vol. 75 (1970).
5. J. B. Goodenough, "Magnetism and the Chemical Bond," Wiley, New York (1963).
6. H. M. Rietveld, *J. Appl. Crystallogr.* **2,** 65 (1969).
7. P. C. Donohue and E. L. McCann, *Mater. Res. Bull.* **12,** 519 (1977).
8. J. Krüger and H. Müller-Buschbaum, *Zeit. Anorg. Allg. Chem.* **512,** 59 (1984).
9. H. Müller-Buschbaum and R. von Schenk, *Zeit. Anorg. Allg. Chem.* **377,** 70 (1970).
10. J. M. Longo, P.M. Raccah, and J. B. Goodenough, *J. Appl. Phys.* **39,** 1327 (1968).